Langmuir
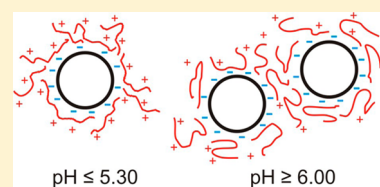
Insights on the Interactions of Chitosan with Phospholipid Vesicles. Part I: Effect of Polymer Deprotonation

Omar Mertins*,[†] and Rumiana Dimova*

Department of Theory and Bio-Systems, Max Planck Institute of Colloids and Interfaces, Science Park Golm, 14424 Potsdam, Germany

S *Supporting Information*

ABSTRACT: Interactions between the polysaccharide chitosan and negatively charged phospholipid liposomes were studied as a function of compositional and environmental conditions. Using isothermal titration calorimetry, different levels of deprotonation of chitosan in acidic solutions were attained with titration of the fully protonated polymer at pH 4.48 into solutions with increasing pH. The process was found to be highly endothermic. We then examined the interaction of the polymer with vesicles in solutions of different pH. Even when partially deprotonated, the chitosan chains retain their affinity to the negatively charged liposomes. However, the stronger adsorption results in lower organization of the chains over the membrane.

pH ≤ 5.30   pH ≥ 6.00

1. INTRODUCTION

Lipid vesicles represent a variety of colloidal structures formed by the self-assembly of phospholipid molecules into bilayers. Liposomes with sizes in the 100 nm range are probably the most studied and well developed example of nanovesicles applied as advanced drug delivery systems.[1−10]

Chitosan is a well-known polysaccharide, obtained from deacetylation of natural chitin which is the main component of crustacean shells. Currently, chitosan is being considered as an important biocompatible macromolecule[11] extensively used for the development of drug and vaccine carriers aiming to optimize efficiency of treatments and achieve controlled antigen release.[12−20] The polymer is soluble in aqueous solutions with pH lower than 5.5 as a result of protonation of the amino groups along the polymer chain; see Figure 1A. The protonation results in an extended polyelectrolyte which can exhibit strong interactions with phospholipids in model and cellular membranes[21−26] as well as with negatively charged surfaces.[27] Hence, the mucoadhesive property of chitosan has been explored in the development of chitosomes (liposomes modified with chitosan) with the aim not only to target drug carriers to specific sites of action, but also to further prolong the drug therapeutic action by keeping the vesicles adsorbed over the cell membranes for increased periods of time.[28,29]

Nevertheless, the well-known instability of drug delivery systems in biological media prevents the efficiency of the carriers. Thus, the development of such systems requires detailed knowledge of all physical, chemical, and biological characteristics playing a role in processes involved at many levels, starting from the production to the final in vivo performance. In what concerns liposomes modified with chitosan, in the recent years, deeper understanding has been gained on fundamental aspects related to the vesicle preparation method,[30] physical and morphological features,[31,32] stability parameters under temperature variation,[33] and

molecular interactions.[34] The applicability of these vesicles as a vaccine delivery system has also been evaluated.[12,14] More recently, we have studied the thermodynamic characteristics of the binding of chitosan onto the membranes of liposomes made of zwitterionic phospholipids and different fractions of negatively charged phospholipids.[35] The electrostatic interactions between the macromolecules and the membrane were found to be regulated by and to increase with the vesicles surface charge. At the point of saturation via charge compensation, the vesicles were shown to aggregate. The role of polymer charge, that is, degree of deionization or deprotonation, was not investigated.

To further elucidate the processes occurring during the encounter of chitosan with phospholipids vesicles, our purpose in the present report was to explore the effect of deprotonation of the polymer amino groups as a driving force governing the interaction. We first studied in more detail and thermodynamically characterized the deprotonation of chitosan introduced in solutions of various pH. We then performed a thorough investigation of the effect of deprotonation on the polymer stability and interaction with partially charged lipid vesicles. Having characterized the properties of the system from the viewpoint of the polysaccharide, in a following study, we pursued the characterization of the membrane response in terms of mechanical properties and stability upon contact with chitosan.[36]

2. MATERIALS AND METHODS

2.1. Materials. Chloroform solutions of 1,2-dioleoyl-*sn*-glycero-3-phosphatidylcholine (DOPC) and 1,2-dioleoyl-*sn*-glycero-3-phosphatidylglycerol (sodium salt) (DOPG) were purchased from Avanti Polar

Lipids Inc. (Birmingham, AL) and used without further purification. They were stored at −20 °C upon arrival. Chitosan was a gift from Primex (Germany), with 95% degree of deacetylation (DDA). The average molecular weight was determined as M_w = 199 kDa (corresponding to 1223 repeat monomers per molecule) by multiangle laser light scattering size exclusion chromatography (MALLS-SEC),[37] with a radius of gyration of 46 nm.

All other reagents were of analytical grade. All solutions were prepared using deionized water from Milli-Q Millipore system with a total organic carbon value of less than 15 ppb and a resistivity of 18 MΩ cm.

2.2. Preparation of Large Unilamellar Vesicles (LUVs) and Chitosan Solutions. The lipid solutions in chloroform were transferred into round-bottom flasks, and the organic solvent was removed by evaporation under a stream of nitrogen gas until complete drying followed by 2 h in a vacuum desiccator. An aqueous buffer solution of acetic acid/sodium acetate was added in the flask with the lipid film. All buffers were prepared at a total concentration of 80 mM, but varying weight fractions of acid and salt in order to obtain the desired pH: 4.90, 5.30, 6.00, or 7.10 with a maximal variation of 0.01. Liposomes were obtained by vortexing for about 2 min, followed by extrusion using a LipsosoFast pneumatic extruder (Avestin Inc., Ottawa, Canada) operating at a pressure of 200 kPa. The final total lipid concentration in all experiments was 3.82 mM and the molar ratio between DOPC and DOPG was adjusted to obtain negatively charged vesicles with 10 mol % DOPG (0.38 mM). The extrusion was performed in three consecutive steps: 20 times extrusion through a 400 nm diameter pore polycarbonate filter, 20 times through a 200 nm diameter pore filter, and finally 40 times through a 100 nm diameter pore filter. Vesicles prepared in this way generally have a narrow size distribution as confirmed with dynamic light scattering (PDI around 1.5) and are known to be almost entirely unilamellar.[38]

The chitosan solution was prepared by vigorous overnight stirring of the powder in the acetate buffer (pH 4.48 ± 0.01), at a concentration of 1 mg/mL. Solutions with lower concentrations were prepared by diluting the stock solution with buffer. The pH of all solutions was constantly monitored before and after sample preparation and the conductivity was measured, to ensure constant ionic strength. Acetic acid was carefully added to adjust the pH when required.

2.3. Dynamic Light Scattering and ζ-Potential. Size distribution measurements on chitosan solutions and LUV suspensions were performed with Zetasizer Nano ZS instrument (Malvern Instruments, Worcestershire, U.K.). The instrument uses a 4 mW HeNe laser at a wavelength of 632.8 nm and detection at an angle of 173°. All measurements were performed in a temperature controlled chamber at 25 °C. The autocorrelation function was acquired using exponential spacing of the correlation time. The data analyses were performed with software provided by Malvern. The intensity-weighted size distribution was obtained by fitting data with a discrete Laplace inversion routine.[39]

The ζ-potential of vesicles and chitosan was analyzed in the same Malvern Zetasizer instrument performing at least six runs per sample. The measurement principle is based on laser Doppler velocimetry. The electrophoretic mobility u is converted to ζ-potential using the Helmholtz−Smoluchowski relation $\zeta = u\eta/\varepsilon\varepsilon_0$, where η is the solution viscosity, ε the dielectric constant of water, and ε_0 the permittivity of free space.

2.4. Isothermal Titration Calorimetry (ITC). ITC measurements were performed with a VP-ITC microcalorimeter from MicroCal Inc. (Northampton, MA). The working cell (1.442 mL in volume) was filled with the LUV suspension, and the reference cell with the corresponding liposome-free buffer solution. One aliquot of 2 μL followed by 27 aliquots of 10 μL of chitosan solution (pH 4.48 ± 0.01) were injected stepwise with 200 s intervals into the working cell filled with the vesicle suspension of variable pH, namely, 4.90, 5.30, 6.00, and 7.10 (±0.01). The corresponding reference experiments were also performed, that is, titration of chitosan-free buffer in vesicle suspension and titration of chitosan solution in vesicle-free buffer. To avoid the presence of bubbles, all samples were degassed for 10 min shortly before performing the measurements. The sample cell was constantly

stirred at a rate of 307 rpm, and the measurements were performed at 25 °C. The data analyses were carried out with Origin software provided by MicroCal.

3. RESULTS AND DISCUSSION

3.1. Chitosan Deprotonation. Intuitively, electrostatic interactions are first to consider when discussing binding of the positively charged chitosan to negatively charged vesicles. Considering the dimensions of the (small) vesicles and the long chitosan backbone, the polymer has to bend when adsorbing to the LUV membrane, altering the surface charge of the vesicles. Apart from these effects, we considered another factor promoting the interaction between the two identities, namely, the deprotonation of the chitosan chains or, in other words, the transfer of protons from some amino groups to the solution. Deprotonation was found to play a role in the binding of chitosan to DNA.[40] Associated effects may be insignificant in conditions where chitosan is permanently protonated, that is, in a good solvent. However, in a bad solvent, this effect must be taken into account, considering that the structure and solubility of chitosan is strongly influenced by the pH of the solution.[41]

To promote deprotonation of chitosan, in the titration measurements, the pH of the liposome suspension was increased from 4.48 ± 0.01 to 7.10 ± 0.01. The pH of the original chitosan solution was kept constant at 4.48 ± 0.01. In this way, when fully (100%) protonated chitosan at pH 4.48 is titrated in liposome suspension with higher pH, some amino groups must deprotonate.

On its own, the deprotonation of chitosan is strongly endothermic, that is, producing strong endothermic titration peaks as shown in Figure 1B. The polymer was titrated in a
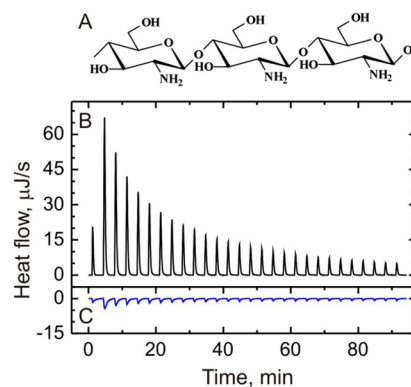
Figure 1. Molecular structure of deionized/deprotonated chitosan (A). Isothermal titration calorimetry traces (25 °C) for the titration of chitosan solution at concentration of 1 mg/mL (6.13 mM of monomers) at pH 4.48 ± 0.01 (80 mM acetate buffer) in the same buffer at pH 7.10 ± 0.01 (B), and for the titration of chitosan-free buffer with pH 4.48 into the corresponding buffer at pH 7.10 (C). The exothermic heat contribution due to buffer mixing is small (less than 10% in magnitude) compared to the endothermic heat of chitosan dilution.

buffer with pH 7.10 in the absence of vesicles. Even very slight differences in pH produce high endothermic signal when the pH is higher than that of the chitosan solution. The reference titration reflecting the contribution of buffer ionization is also shown, see Figure 1C, where the chitosan-free buffer at pH 4.48 was injected into the buffer at pH 7.10. The heat signal of this buffer mixing is exothermic and small in magnitude (less than 10%) compared to the heat absorbed upon chitosan dilution.

Titrations in buffers with pH 4.90, 5.30, and 6.00 have shown qualitatively similar results (data not shown).

To understand the nature of the strong endothermic signal associated with the dilution of protonated chitosan in buffers with higher pH, we first consider pure dilution of the polymer. In a previous study,[35] we have shown that the injection of chitosan solution into the same (native) buffer solution (with identical pH), produces composite peaks. Each injection consists of a small exothermic peak immediately followed by an endothermic one, resulting in an overall endothermic signal of only around 2 μJ per injection; see also Figure S1 in the Supporting Information. However, as shown in Figure 1B, the simple dilution of the fully protonated polysaccharide in a solution with increased pH results in strong endothermic effect. The signal is more than 2 orders of magnitude higher; compare with data in Figure S1 in the Supporting Information. This behavior must be associated with deprotonation of the amino group of the chitosan monomers to reach charge equilibrium in the new solvent. The deprotonation of the polymer is also evidenced from the decrease in the ζ-potential measured in solutions of increasing pH; see Table 1. Further contributions

Table 1. Chitosan Characteristics in the Native Buffer at pH 4.48 ± 0.01 and after Titration in 80 mM Acetate Buffer of Different pH[a]

initial pH	final pH	particle diameter (nm)	ζ-potential (±5 mV)	conductivity (mS/cm)
	4.48 (native)	87 ± 26	53	3.92
4.90	4.81	112 ± 36	47	3.86
5.30	5.10	134 ± 33	42	4.13
6.00	5.42	477 ± 182	40	4.41
7.10	5.64	aggregates	40	4.78

[a]The first column indicates the buffer pH before mixing, and the second column shows the conditions after the titration and at which the DLS and ζ-potential measurements were performed. The errors in the particle diameter indicate standard deviations. The standard deviation in the ζ-potential measurements performed on the same sample was less than 1 mV. In the column title, we have indicated the instrument accuracy as specified by the manufacturer. The monomeric concentration of the original chitosan solution was 6.13 mM (95% DDA, 199 kDa). See text for details.

to the heat release in the titration curves may be related to structural changes in the polymer. Indeed, deprotonation of chitosan can be expected to result in conformational changes, whereby the extended chains may bend and fold adopting a new organization in order to reduce the contact with the polar water molecules. Such structural changes can produce endothermic signal resulting from delocalization of water molecules and deprotonation, both taking place as the conformation of the polymer is changing. Another effect to be considered above a certain degree of deprotonation is the aggregation of the polymer in solutions with higher pH. Evidence for aggregation is provided from dynamic light scattering (DLS); see Table 1. The measured size increases systematically after titration in solutions with increasing pH. Titration in buffer with pH 6.00 leads to a more pronounced size increase, while in solutions of pH 7.10 micrometric particles were detected.

Whenever pH values of solutions are adjusted, one typically adds small amounts of strong acid, which may significantly alter the ionic strength of the solution and consequently affect the electrostatic interactions. In the measurements above, we took extra care to carefully adjust the pH to avoid strong variations in the ionic strength. For monitoring purposes, we measured the solutions conductivities to make sure that the ionic strength of the solutions did not vary significantly; see last column in Table 1. Solutions with excessively high deviations in the conductivity, more than around 0.7 mS/cm compared to the average value, were discarded as they would correspond to a change in the ionic strength by more than around 10 mM.

When two buffers are mixed in titration, both bear a buffering effect, which leads to a different pH of equilibrium as indicated in the second column of Table 1. Hence, the associated heat absorption is higher in the first injections (Figure 1B), where the pH difference between the mixed solutions is maximal. Subsequently, the signal decreases after each new injection, meaning that the new polymer chains introduced in the buffer with the following injections suffer less deprotonation than the chains from the previous injections, as a consequence of pH reduction from the buffering effect.

To summarize, the heat release in the ITC measurements can be ascribed to the combined effect of different contributions, namely, deprotonation of amino groups, changes in polymer conformation, and polysaccharide aggregation. All these effects are more pronounced when the change in pH is larger.

3.2. Interaction of Deprotonated Chitosan with Liposomes. Having characterized the effects associated with

Table 2. Results for the ζ-Potential and the Hydrodynamic Diameter of DOPC/DOPG Liposomes (90/10, 3.82 mM total phospholipid concentration in 80 mM acetate buffer) in Buffers of Varied pH at 25 °C after Titration with the 80 mM Acetate Buffer with Constant pH of 4.48 and after Titration with Chitosan Solution (6.13 mM of monomers in 80 mM acetate buffer, pH 4.48)[a]

| | | | | | titration of buffered chitosan in vehicles | | | |
| | | | titration of buffer in vesicles | | | | degree of deprotonation (1 − α) (%) | |
vesicle pH	pH of added solution	final pH	ζ-potential (±5 mV)	particle diameter (nm)	ζ-potential (±5 mV)	particle diameter (nm)	first injection	final injection
4.90	4.48	4.82	−26	93 ± 3	41	223 ± 14	7	6
5.30	4.48	5.11	−29	103 ± 4	39	239 ± 23	17	11
6.00	4.48	5.43	−21	98 ± 4	38	aggregates	50	21
7.10	4.48	5.64	−24	109 ± 3	39	aggregates	93	30

[a]The errors in the particle diameter indicate standard deviations. The standard deviation in the ζ-potential measurements on the same sample was less than 1 mV. In the column title, we have indicated the instrument accuracy as specified by the manufacturer. The calculated percentage of deprotonation degree (1/α) of chitosan for each vesicle pH is shown in the last two columns; see text for details.

253 mixing chitosan with buffers at different pH, we now proceed
254 with discussing the interaction of the polymer with the
255 membrane. As a charged model membrane, we have chosen
256 DOPC vesicles containing 10 mol % DOPG (DOPC/DOPG
257 90/10) since these fractions of charged lipid have yielded
258 reasonable ITC signal.[35] Furthermore, the pK_a of DOPG is
259 around 3[42,43] which implies that the surface charge of the bare
260 vesicles remains negative after titration of buffer with higher
261 pH. This is confirmed by the ζ-potential measurements given in
262 Table 2, which suggest that the membrane surface charge is not
263 altered when the liposomes get in contact with the native buffer
264 of the chitosan solutions.

265 Figure 2 shows an example titration of chitosan in a vesicle
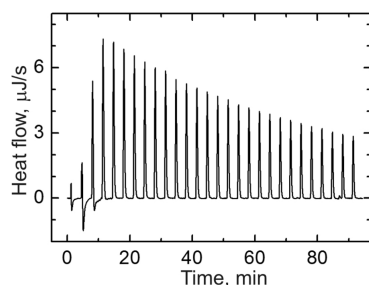266 suspension at pH 5.30. The first few injections produce a

Figure 2. ITC trace (25 °C) for DOPC/DOPG liposomes (90/10, 3.82 mM total phospholipids) at pH 5.30 ± 0.01 (80 mM acetate buffer) titrated with chitosan solution (1 mg/mL, 6.13 mM of monomers) at pH 4.48 ± 0.01 (same acetate buffer).

267 composite signal: a positive (upward) endothermic peak
268 immediately followed by a negative (downward) exothermic
269 peak. The magnitude and trend of the exothermic part of the
270 signal is similar to that observed when titrating the same
271 chitosan solution in the vesicle suspension (DOPC/DOPG 90/
272 10) but at pH 4.48;[35] see Figure S2 in the Supporting
273 Information. This suggests that the exothermic part of the
274 signal is associated with the neutralization of negative charges
275 of DOPG by the positive ionized amino groups of chitosan.
276 However, now the exothermic effect is quickly suppressed by
277 the endothermic signal associated with chitosan deprotonation.
278 After the third injection, the peaks turn highly positive and the
279 endothermic effect predominates until the end of the titration
280 with intensity similar to that of the reference titration (titration
281 of chitosan solution in the corresponding vesicle-free buffer,
282 compare with Figure 1B). This trend was observed for all
283 measurements at different pH.

284 After subtracting the reference measurement from the main
285 titration, that is, deducting the effect associated with chitosan
286 dilution and deprotonation, one obtains the net signal
287 associated with polymer-vesicle interaction. In Figure 3, we
288 present the data in terms of integrated heat per injection for
289 every different pH shift. The first injection point is excluded
290 from the data since it is strongly influenced by dilution effects
291 during the pre-equilibration stage of the measurement. The
292 results in Figure 3A are presented in terms of interaction with
293 the accessible lipid considering that chitosan can interact only
294 with the external leaflet of the vesicle membrane because at the
295 explored conditions, no bilayer poration has been observed; see
296 accompanying study.[36] The data show that the heat released
297 from DOPG neutralization is highly exothermic and the signal
298 increases for higher differences in the pH between the chitosan
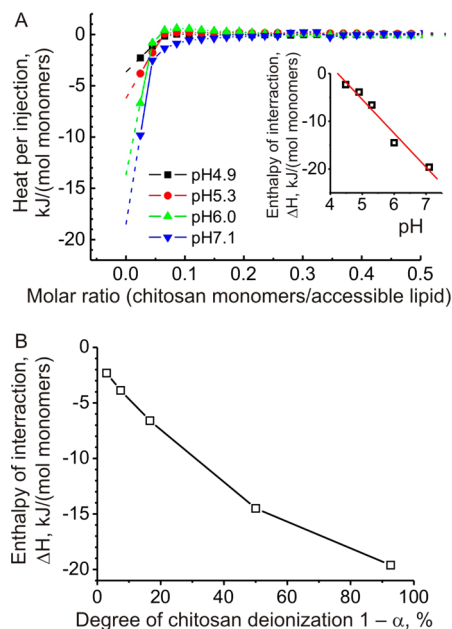299 solution and the vesicle suspension. Above molar ratios of 0.1

Figure 3. (A) Integrated heat per injection versus the molar ratio of chitosan to phospholipids present in the external leaflet of the liposome membrane for the titrations of chitosan solution (1 mg/mL, 6.13 mM monomeric chitosan) at pH 4.48 ± 0.01 (80 mM acetate buffer) in DOPC/DOPG small liposomes (90/10, 3.82 mM total phospholipids) in 80 mM acetate buffers with different pH (±0.01) as indicated. The heat of chitosan dilution has been subtracted from the data. The inset plot shows the decrease in molar enthalpy of polymer–lipid interaction as a function of pH in the solution (the first data point for pH 4.48 is taken from ref 35); see text for details. The slope of the linear fit is (−7.08 ± 0.71) kJ/mol per pH unit. (B) Molar enthalpy of interaction as a function of the degree of deionization (deprotonation) of the polymer calculated for the first injection of the ITC measurement.

300 chitosan monomers-to-accessible lipid, the released heat levels
301 out close to zero for all samples, suggesting, once again,
302 neutralization of DOPG on the membrane of the vesicles (note
303 that the molar fraction of DOPG in the membrane is 10%).
304 However, when varying the pH of the liposome suspension,
305 one has to consider the deprotonation of chitosan as an
306 effective process that influences the interaction of the polymer
307 with the vesicle membrane.

308 We did not pursue model fitting of the titration data sets to
309 extract binding constants because of the relatively weak signal
310 and the lack of strong functional dependence in the explored
311 interval of molar ratios. However, we performed the following
312 rough analysis to evaluate the molar enthalpy of binding. The
313 data was extrapolated to zero molar ratio of chitosan monomers
314 to accessible lipid; see dashed curves in Figure 3A. In this
315 regime of excess lipid, one can assume that all injected chitosan
316 fully engages in binding to the membrane. The released heat
317 will be then directly proportional to the molar enthalpy of
318 interaction, ΔH, and given by the intercept. The inset in Figure
319 3 shows the linear variation of the molar enthalpy ΔH
320 estimated in this way as a function of the pH of the vesicle
321 solutions. The higher the pH, the larger in magnitude the
322 enthalpy of interaction is demonstrating the stronger
323 exothermic effect as a function of increasing pH.

324 Considering the different acidity conditions analyzed in this
325 work, buffers with pH values of 4.90 and 5.30 are still
326 reasonably good solvents for chitosan and when the polymer is

introduced in these buffers only a small amount of protons must be transferred to the solution. However, taking into account the enthalpy deduced for the first injections in solutions of pH values 4.90 and 5.30 (see inset in Figure 3A), it is reasonable to admit that even weak deprotonation of chitosan influences the energy of electrostatic interaction, where the enthalpy changes almost by a factor of 2, from −3.87 kJ/mol of chitosan monomer in pH 4.90 to −6.60 kJ/mol of chitosan monomer in pH 5.30.

On the other hand, the solutions with higher pH values of 6.00 and 7.10 are no longer good solvents for chitosan and deprotonation of the amino groups is largely increased when the polymer is introduced. Chitosan becomes unstable in these buffers and exhibits a critical tendency to form aggregates (Table 1).

Following an approach introduced by Rinaudo et al.,[41] we estimated the degree of deprotonation of chitosan for each pH evaluated in this work using the expression

$$pK_a = pH + \log_{10}[\alpha/(1 - \alpha)]$$

where pK_a for chitosan is assumed to be 6.0[41] and α is the degree of protonation, that is, the opposite of the degree of deprotonation $(1 - \alpha)$. For the native chitosan solution with pH 4.48, the degree of protonation is 97%, or equivalently in terms of deprotonation degree $1 - \alpha = 3\%$. These values imply full solubility of the polymer chains. As expected, with increasing pH, the deprotonation degree increases as evidenced in Table 2. At pH 6.00, it reaches 50%, which is considered the limit for chitosan solubilization.[41] The buffer at pH 7.10 is no longer a good solvent for the polysaccharide, since the deprotonation is higher than 90%.

Let us mention the following caveat here. Such deprotonation degrees may be effective only for the first couple of injections of chitosan solution into the buffers with higher pH. The reason for this is because both solutions have a buffering effect, as discussed above, and their mixing produces a solution with final pH at the end of the titration, also shown in Table 2. Thus, following the first injections, deprotonation of chitosan still occurs, but evidently to a lesser extent since the pH in the titration cell is slowly decreasing with each new injection.

Simultaneously with the polymer deprotonation, the neutralization of negative charges on the membrane of the vesicles containing 10% DOPG also occurs during the first injections of chitosan solution. We consider an approximated deprotonation degree at this point, as given in the penultimate column of Table 2. When injected into the vesicle suspension, the polymer binds onto the negatively charged membranes (note that the membrane surface charge is independent of pH; see Table 2) and an exothermic signal from electrostatic interaction is released indicating stabilization of the system. The higher the difference in pH, and thus the instability of chitosan due to deprotonation, the higher the enthalpic contribution upon binding will be as the polymer acquires stability on the vesicle surface, as shown in Figure 3B. Thus, it is evidenced that the state of lower energy for the system is when chitosan is adsorbed on the membrane of the vesicles instead of being free in solution and in a bad solvent.

After the neutralization of DOPG, basically only endothermic heat of deprotonation of the polymer chains characterizes the system. Once again, the decrease in the endothermic signal for each subsequent injection of chitosan solution observed in Figures 1B and 2 is related to the systematic reduction of pH in the ITC reaction cell due to the addition of increasing amounts of chitosan buffer at pH 4.48. As shown in Table 2, the final pH in the cell is around 5 depending on the initial pH of the vesicles buffer. In this way, the decrease in the endothermic signal also shows the decrease of chitosan deprotonation as a function of pH.

Let us now consider the results for the ζ-potential and particle size in the deprotonation experiments. The data given in Table 2 evidence that simple titration of chitosan-free buffer with pH 4.48 into vesicle suspensions with increasing pH values produces neither a change in the size nor in the ζ-potential of the bare vesicles. All vesicles remain with around 100 nm of hydrodynamic diameter and surface charge close to −25 mV. After titration with chitosan solution, the vesicles in solutions of pH 4.90 and 5.30 behave similarly exhibiting a substantial increase in size and ζ-potential, suggesting chitosan adsorption. However, the vesicles in solutions at pH 6.00 and 7.10 show the presence of microaggregates after titration with chitosan, but no further increase in the ζ-potential. Thus, the adsorption of chitosan on the membrane of small liposomes may be influenced also by the degree of deprotonation of the polymer.

To summarize, the adsorption of polymer chains on the liposomes is irreversible and alters the vesicle membrane characteristics. The mechanical properties of the membranes are also significantly altered as explored in the subsequent study employing giant vesicles.[36] Indeed, the aggregation observed here by means of the DLS measurements may be responsible for increasing the membrane apparent roughness as visualized with microscopy observations on giant vesicles incubated in chitosan solutions. The change in surface charge from negative for the bare vesicles to positive for the chitosomes might be responsible for the observed adhesion and rupture of giant vesicle in contact with glass surfaces.[36]

3.3. Polymer Reorganization. Previously, we have proposed a model to explain the organization of the electrostatically driven binding of chitosan onto liposomes with varied surface charge.[35] Here, we discuss a model to address the reorganization of the polymer under the effect of deprotonation. As illustrated in Figure 4A, for pH values lower
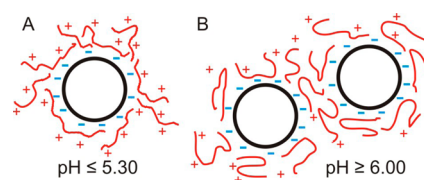
Figure 4. Schematic representation of chitosome structures. (A) Positively charged chains of chitosan are attracted by the slightly negative surface charge of the small liposome in buffer with pH ≤ 5.30. (B) Aggregates of chitosomes formed after the partial deprotonation of chitosan in buffer with pH ≥ 6.00. The polymer chains bind to the membrane of the slightly negatively charged liposomes and mediate adhesion based on hydrophobic attraction between the deionized/deprotonated parts of chitosan. The overall surface charge becomes positive; see text for details.

and around 5.30 where the deprotonation of chitosan is low, the polymer chains are attracted by the slightly negatively charged DOPC/DOPG 90/10 vesicles and adsorption must occur in a similar fashion as previously described for these structures. As a consequence of the adsorption of the bulky polymer chains, the chitosome size increases and the ζ-potential becomes highly positive, preventing aggregation (Table 2).

In solutions with pH 6.00 and above, the deprotonation of chitosan is increased (Table 2) and the polymer is no longer stable in the buffer. The negative charges on the vesicles are available in the same buffer and chitosan is strongly attracted, leading to stronger adsorption as shown by the increased exothermic heat release when comparing the ITC data collected for different pH values; see Figure 3B. The stronger attraction which has to occur fast (and mainly in the first injections) may lead to lower organization of the polymer over the membrane, leading to chitosome aggregates once again, as discussed before.[35] However, since the surface charge of the DOPC/DOPG 90/10 vesicles is only slightly negative, the final ζ-potential turns now positive (Figure 4B), contrary to what was observed for vesicles with higher DOPG fractions.[35] In addition, as a consequence of deprotonation of chitosan, hydrophobic domains are produced on the chains presumably leading to changes in the conformation of the polymer as a result of intramolecular and intermolecular hydrophobic interactions.[27] Furthermore, the deionized/deprotonated segments of the chains must have looser binding over the membrane of the vesicles, since electrostatic interaction with these segments is no longer possible. Thus, for pH ≥ 6.00, one could expect that upon adsorption to the liposome surface the polymer chains attain conformations, which differ from those at lower pH as illustrated in Figure 4. Differently from the previous report,[35] where the aggregation may be produced by looser chains attracted by the strong negative charge of neighboring vesicles, in the present study, the net charge is no longer negative as shown by the increase in ζ-potential (Table 2), suggesting that now the aggregation is caused mainly by hydrophobic interactions between the deprotonated loops of the looser chains.

To summarize, the deprotonation of chitosan at high pH leads to polymer reorganization that strongly influences the interaction and adsorption of the chains on the liposome membranes. For the intermediate pH values, between 5.30 and 6.00, the chitosan behavior in solution is difficult to evaluate and more effort has to be made in this direction. In this pH range, the polymer solubility changes significantly as the degree of deprotonation increases and intramolecular interactions appear to influence the conformation of the polymer. The polymer behavior may also be influenced by the distribution of remaining acetyl groups as well as by the distribution of molecular weight, as chitosan behavior in such solutions is far from ideal.[40]

In order to better understand the polysaccharide−membrane interaction and enlighten the physical characteristics associated with the encounter of chitosan with phospholipid membranes, we addressed the effect of the polymer on the membrane rigidity and pore formation in giant unilamellar vesicles with similar lipid composition.[36]

4. CONCLUDING REMARKS

The interaction between chitosan and phospholipid vesicles may be enhanced by means of altering compositional and environmental conditions. Here, we demonstrated the use of chitosan deprotonation as a tool to modulate the polymer adsorption to the membrane. The deprotonation of chitosan was promoted with titration of the protonated polymer into solutions with increasing pHs and the process was found highly endothermic. This endothermic effect increases with pH showing that the chitosan structure and behavior are strongly dependent on the media acidity. Partially deionized/deproto-

nated chains still exhibit affinity to the negative surface charges of the membrane. Further deprotonation of the polymer seems not to lead to weaker affinity. Indeed, when bound, chitosan reaches higher stability compared to when it remains free in a poorly protonating solvent, a fact that was shown by the exothermic signal in the ITC titration. However, it has to be stressed that, once again, stronger adsorption results in lower organization of the polymer chains over the membrane. This lower organization, in addition to conformational changes of the chains due to deprotonation, also promotes aggregation of the chitosome structures. Since the final surface charge on chitosomes is highly positive in this case, hydrophobic interactions between deprotonated looser loops of chitosan segments must be related to the aggregation process.

The findings of the present study highlight the importance of degree of chitosan protonation in research areas where chitosan is employed as a macromolecule for biological and biomedical applications. More specifically, the mucoadhesive properties of liposomes coated with chitosan, intended as specific drug delivery systems, may be improved with the knowledge about the degree of chitosan protonation. The polymer deprotonation will influence the degree of coverage in these coated liposomes and can be used to modulate it. In a following study,[36] we demonstrate that, on giant vesicles, this coverage is very heterogeneous and depends on the preparation protocol employed.

■ ASSOCIATED CONTENT

Ⓢ Supporting Information

ITC data. This material is available free of charge via the Internet at http://pubs.acs.org.

■ AUTHOR INFORMATION

Corresponding Authors
*E-mail: Mertins@if.usp.br.
*E-mail: Rumiana.Dimova@mpikg.mpg.de.

Present Address
†O.M.: Department of Applied Physics, Institute of Physics, University of Sao Paulo, Rua do Matao, Travessa R 187, 05508-090 Sao Paulo, Brazil.

Notes
The authors declare no competing financial interest.

■ REFERENCES

(1) Lasic, D. D. Doxorubicin in Sterically Stabilized Liposomes. *Nature* **1996**, *380*, 561−562.

(2) Immordino, M. L.; Dosio, F.; Cattel, L. Stealth liposomes: Review of the Basic Science, Rationale, and Clinical Applications, Existing and Potential. *Int. J. Nanomed.* **2006**, *1* (3), 297−315.

(3) Gunaseelan, S.; Gunaseelan, K.; Deshmukh, M.; Zhang, X.; Sinko, P. J. Surface Modifications of Nanocarriers for Effective Intracellular Delivery of anti-HIV Drugs. *Adv. Drug Delivery Rev.* **2010**, *62* (4−5), 518−531.

(4) Kuijpers, S. A.; Coimbra, M. J.; Storm, G.; Schiffelers, R. M. Liposomes Targeting Tumour Stromal Cells. *Mol. Membr. Biol.* **2010**, *27* (7), 328−340.

(5) Singh, S. Nanomedicine-Nanoscale Drugs and Delivery Systems. *J. Nanosci. Nanotechnol.* **2010**, *10* (12), 7906−7918.

(6) Hua, S.; Chang, H.; Davies, N. M.; Cabot, P. J. Targeting of ICAM-1-Directed Immunoliposomes Specifically to Activated Endothelial Cells with Low Cellular Uptake: Use of an Optimized Procedure for the Coupling of Low Concentrations of Antibody to Liposomes. *J. Liposome Res.* **2011**, *21* (2), 95−105.

(7) Muthu, M. S.; Kulkarni, S. A.; Xiong, J.; Feng, S.-S. Vitamin E TPGS Coated Liposomes Enhanced Cellular Uptake and Cytotoxicity of Docetaxel in Brain Cancer Cells. *Int. J. Pharm.* **2011**, *421* (2), 332−340.

(8) Chandrawati, R.; Caruso, F. Biomimetic Liposome- and Polymersome-Based Multicompartmentalized Assemblies. *Langmuir* **2012**, *28* (39), 13798−13807.

(9) Pozza, E. D.; Lerda, C.; Costanzo, C.; Donadelli, M.; Dando, I.; Zoratti, E.; Scupoli, M. T.; Beghelli, S.; Scarpa, A.; Fattal, E.; Arpicco, S.; Palmieri, M. Targeting Gemcitabine Containing Liposomes to CD44 Expressing Pancreatic Adenocarcinoma Cells Causes an Increase in the Antitumoral Activity. *Biochim. Biophys. Acta, Biomembr.* **2013**, *1828* (5), 1396−1404.

(10) Zhao, Y.; Alakhova, D. Y.; Kim, J. O.; Bronich, T. K.; Kabanov, A. V. A Simple Way to Enhance Doxil Therapy: Drug Release from Liposomes at the Tumor Site by Amphiphilic Block Copolymer. *J. Controlled Release* **2013**, *168* (1), 61−69.

(11) Aranaz, I.; Mengíbar, M.; Harris, R.; Paños, I.; Miralles, B.; Acosta, N.; Galed, G.; Heras, A. Functional Characterization of Chitin and Chitosan. *Curr. Chem. Biol.* **2009**, *3*, 203−230.

(12) Marón, L. B.; Covas, C. P.; da Silveira, N. P.; Pohlmann, A.; Mertins, O.; Tatsuo, L. N.; Sant'Anna, O. A. B.; Moro, A. M.; Takata, C. S.; de Araujo, P. S.; Bueno da Costa, M. H. LUVs Recovered with Chitosan: A New Preparation for Vaccine Delivery. *J. Liposome Res.* **2007**, *17* (3−4), 155−163.

(13) Guo, R.; Zhang, L. Y.; Qian, H. Q.; Li, R. T.; Jiang, X. Q.; Liu, B. R. Multifunctional Nanocarriers for Cell Imaging, Drug Delivery, and Near-IR Photothermal Therapy. *Langmuir* **2010**, *26* (8), 5428−5434.

(14) Rescia, V. C.; Takata, C. S.; de Araujo, P. S.; Bueno da Costa, M. H. Dressing Liposomal Particles with Chitosan and Poly(vinylic alcohol) for Oral Vaccine Delivery. *J. Liposome Res.* **2011**, *21* (1), 38−45.

(15) Venkatesan, P.; Puvvada, N.; Dash, R.; Kumar, B. N. P.; Sarkar, D.; Azab, B.; Pathak, A.; Kundu, S. C.; Fisher, P. B.; Mandal, M. The Potential of Celecoxib-Loaded Hydroxyapatite-Chitosan Nanocomposite for the Treatment of Colon Cancer. *Biomaterials* **2011**, *32* (15), 3794−3806.

(16) Gonçalves, M. C. F.; Mertins, O.; Pohlmann, A. R.; Silveira, N. P.; Guterres, S. S. Chitosan Coated Liposomes as an Innovative Nanocarrier for Drugs. *J. Biomed. Nanotechnol.* **2012**, *8* (2), 240−250.

(17) Gordon, S.; Young, K.; Wilson, R.; Rizwan, S.; Kemp, R.; Rades, T.; Hook, S. Chitosan Hydrogels Containing Liposomes and Cubosomes As Particulate Sustained Release Vaccine Delivery Systems. *J. Liposome Res.* **2012**, *22* (3), 193−204.

(18) Jose, S.; Fangueiro, J. F.; Smitha, J.; Cinu, T. A.; Chacko, A. J.; Premaletha, K.; Souto, E. B. Cross-Linked Chitosan Microspheres for Oral Delivery of Insulin: Taguchi Design and in Vivo Testing. *Colloids Surf., B* **2012**, *92*, 175−179.

(19) Calderón, L.; Harris, R.; Cordoba-Diaz, M.; Elorza, M.; Elorza, B.; Lenoir, J.; Adriaens, E.; Remon, J. P.; Heras, A.; Cordoba-Diaz, D. Nano and Microparticulate Chitosan-Based Systems for Antiviral Topical Delivery. *Eur. J. Pharm. Sci.* **2013**, *48* (1−2), 216−222.

(20) Sanyakamdhorn, S.; Agudelo, D.; Tajmir-Riahi, H.-A. Encapsulation of Antitumor Drug Doxorubicin and Its Analogue by Chitosan Nanoparticles. *Biomacromolecules* **2013**, *14* (2), 557−563.

(21) Fang, N.; Chan, V.; Mao, H. Q.; Leong, K. W. Interactions of Phospholipid Bilayer with Chitosan: Effect of Molecular Weight and pH. *Biomacromolecules* **2001**, *2* (4), 1161−1168.

(22) Mertins, O.; da Silveira, N. P.; Pohlmann, A. R.; Schroder, A. P.; Marques, C. M. Electroformation of Giant Vesicles from an Inverse Phase Precursor. *Biophys. J.* **2009**, *96* (7), 2719−2726.

(23) Krajewska, B.; Wydro, P.; Kyziol, A. Chitosan as a Subphase Disturbant of Membrane Lipid Monolayers. The Effect of Temperature at Varying pH: I. DPPG. *Colloids Surf., A* **2013**, *434*, 349−358.

(24) Young, D. H.; Kohle, H.; Kauss, H. Effect of Chitosan on Membrane-Permeability of Suspension-Cultured Glycine-Max and Phaseolus-Vulgaris Cells. *Plant Physiol.* **1982**, *70* (5), 1449−1454.

(25) Young, D. H.; Kauss, H. Release of Calcium from Suspension-Cultured Glycine-Max Cells by Chitosan, Other Polycations, and Polyamines in Relation to Effects on Membrane-Permeability. *Plant Physiol.* **1983**, *73* (3), 698−702.

(26) Helander, I. M.; Nurmiaho-Lassila, E. L.; Ahvenainen, R.; Rhoades, J.; Roller, S. Chitosan Disrupts the Barrier Properties of the Outer Membrane of Gram-Negative Bacteria. *Int. J. Food Microbiol.* **2001**, *71* (2−3), 235−244.

(27) Claesson, P. M.; Ninham, B. W. pH-Dependent Interactions between Adsorbed Chitosan Layers. *Langmuir* **1992**, *8* (5), 1406−1412.

(28) Takeuchi, H.; Yamamoto, H.; Niwa, T.; Hino, T.; Kawashima, Y. Enteral Absorption of Insulin in Rats from Mucoadhesive Chitosan-Coated Liposomes. *Pharm. Res.* **1996**, *13* (6), 896−901.

(29) Takeuchi, H.; Matsui, Y.; Sugihara, H.; Yamamoto, H.; Kawashima, Y. Effectiveness of Submicron-Sized, Chitosan-Coated Liposomes in Oral Administration of Peptide Drugs. *Int. J. Pharm.* **2005**, *303* (1−2), 160−170.

(30) Mertins, O.; Sebben, M.; Pohlmann, A. R.; da Silveira, N. P. Production of Soybean Phosphatidylcholine-Chitosan Nanovesicles by Reverse Phase Evaporation: A Step by Step Study. *Chem. Phys. Lipids* **2005**, *138* (1−2), 29−37.

(31) Mertins, O.; Cardoso, M. B.; Pohlmann, A. R.; da Silveira, N. P. Structural Evaluation of Phospholipidic Nanovesicles Containing Small Amounts of Chitosan. *J. Nanosci. Nanotechnol.* **2006**, *6* (8), 2425−2431.

(32) Lionzo, M.; Mertins, O.; Pohlmann, A. R.; da Silveira, N. P. Phospholipid/Chitosan Self-Assemblies Analyzed by SAXS and Light Scattering. *Synchrotron Radiat. Mater. Sci.* **2009**, *1092*, 127−129.

(33) Mertins, O.; Lionzo, M. I. Z.; Micheletto, Y. M. S.; Pohlmann, A. R.; da Silveira, N. P. Chitosan Effect on the Mesophase Behavior of Phosphatidylcholine Supramolecular Systems. *Mater. Sci. Eng., C* **2009**, *29* (2), 463−469.

(34) Mertins, O.; Schneider, P. H.; Pohlmann, A. R.; da Silveira, N. P. Interaction between Phospholipids Bilayer and Chitosan in Liposomes Investigated by P-31 NMR Spectroscopy. *Colloids Surf., B* **2010**, *75* (1), 294−299.

(35) Mertins, O.; Dimova, R. Binding of Chitosan to Phospholipid Vesicles Studied with Isothermal Titration Calorimetry. *Langmuir* **2011**, *27* (9), 5506−5515.

(36) Mertins, O.; Dimova, R. Insights on the Interactions of Chitosan with Phospholipid Vesicles. Part II: Membrane Stiffening and Pore Formation. *Langmuir* **2013**, DOI: 10.1021/la4032199.

(37) Godderz, L. J.; Peak, M. M.; Rodgers, K. K. Analysis of Biological Macromolecular Assemblies Using Static Light Scattering Methods. *Curr. Org. Chem.* **2005**, *9* (9), 899−908.

(38) MacDonald, R. C.; MacDonald, R. I.; Menco, B. P. M.; Takeshita, K.; Subbarao, N. K.; Hu, L. R. Small-Volume Extrusion Apparatus for Preparation of Large, Unilamellar Vesicles. *Biochim. Biophys. Acta* **1991**, *1061* (2), 297−303.

(39) Pereira-Lachataignerais, J.; Pons, R.; Panizza, P.; Courbin, L.; Rouch, J.; Lopez, O. Study and Formation of Vesicle Systems with Low Polydispersity Index by Ultrasound Method. *Chem. Phys. Lipids* **2006**, *140* (1−2), 88−97.

(40) Ma, P. L.; Lavertu, M.; Winnik, F. M.; Buschmann, M. D. New Insights into Chitosan-DNA Interactions Using Isothermal Titration Microcalorimetry. *Biomacromolecules* **2009**, *10* (6), 1490−1499.

(41) Rinaudo, M.; Pavlov, G.; Desbrieres, J. Solubilization of Chitosan in Strong Acid Medium. *Int. J. Polym. Anal. Charact.* **1999**, *5* (3), 267−276.

(42) Sacre, M. M.; Tocanne, J. F. Importance of Glycerol and Fatty-Acid Residues on Ionic Properties of Phosphatidylglycerols at Air-Water-Interface. *Chem. Phys. Lipids* **1977**, *18* (3−4), 334−354.

691 (43) Watts, A.; Harlos, K.; Maschke, W.; Marsh, D. Control of
692 Structure and Fluidity of Phosphatidylglycerol Bilayers by pH
693 Titration. *Biochim. Biophys. Acta* **1978**, *510* (1), 63−74.